

Chapter 2

Dimensionless Evaluation of Cell Deformability with High Resolution Positioning in a Microchannel

Chia-Hung Dylan Tsai, Shinya Sakuma, Fumihito Arai and Makoto Kaneko

Abstract This chapter covers dimensionless evaluation for the stiffness-based deformability of a cell using a high-resolution vision system and a microchannel. In conventional approaches, the transit time of a cell through a microchannel is often utilized for the evaluation of cell deformability. However, such time includes both the information of cell stiffness and viscosity. In this work, we eliminate the effect from cell viscosity, and focus on the cell stiffness only. We find that the velocity of a cell varies when enters a channel, and eventually reaches to equilibrium where the velocity becomes constant. The constant velocity is defined as the equilibrium velocity of the cell, and it is utilized to define the observability of stiffness-based deformability. The necessary and sufficient numbers of sensing points for evaluating stiffness-based deformability are discussed. Through the dimensional analysis on the microchannel system, three dimensionless parameters determining stiffness-based deformability are derived, and a new index is introduced based on these parameters. The experimental study is conducted on the red blood cells from a healthy subject and a diabetic patient. With the proposed index, we showed that the experimental data can be nicely arranged.

Keywords Dimensionless evaluation · Cell deformability · Microchannel system · High-speed vision

Part of the materials in this chapter is from C. Tsai, S. Sakuma, F. Arai and M. Kaneko, IEEE Transactions on Biomedical Engineering, vol.61, no.4, pp1187-1195, 2014. The permission of reuse is granted by IEEE.

C.-H. D. Tsai (✉) · M. Kaneko

Department of Mechanical Engineering, Osaka University, Osaka, Japan

e-mail: tsai@hh.mech.eng.osaka-u.ac.jp

S. Sakuma · F. Arai

Department of Micro-Nano Systems Engineering, Nagoya University, Nagoya, Japan

e-mail: sakuma@mech.nagoya-u.ac.jp

M. Kaneko

e-mail: mk@mech.eng.osaka-u.ac.jp

F. Arai

e-mail: arai@mech.nagoya-u.ac.jp

2.1 Introduction

Cell stiffness is important for disease diagnosis based upon known relations with diseases, such as malaria, sepsis, diabetes and etc. [1–4]. For example, Brandao et al. showed that sickle cell anemia causes stiffening of red blood cells (RBCs) [5]. Among all the evaluation methods, microchannel-based methods have a great advantage of high-speed measurement, and it is useful and necessary for obtaining sufficient number of samples regarding the statistical significance of the results. The feature of high-speed measurement is especially important when it comes to practical applications.

In microchannel systems, a cell is deformed to pass through a microchannel whose diameter is smaller than the diameter of the cell, as shown in Fig. 2.1a. Different cell deformabilities result in different cell behaviors during the transits. For example, a cell with low deformability would move slower inside a channel because a greater resistance against the cell motion is generated on the contact between the cell and channel. On the contrary, a cell with high deformability would move faster upon the same consideration. According to this idea, the transit time for a cell through a microchannel is often used as a deformability index (DI) for the evaluation of cell deformability in conventional approaches [6–9].

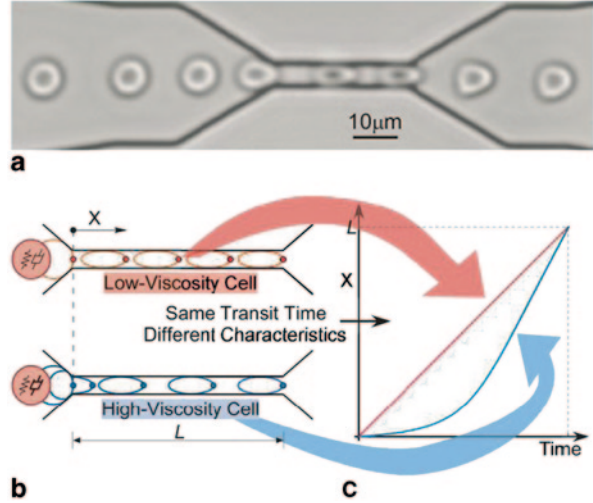
However, we observed that cells with the same transit time sometimes exhibit very different characteristics in terms of motion profiles, as illustrated in Figs. 2.1b and c. Figure 2.1b shows a series of locations of two cells through microchannels. The motion profiles of them are plotted in Fig. 2.1c. The cell on the top of Fig. 2.1b moves at a constant velocity throughout the channel while the lower one starts with acceleration motion, and then moves at a constant velocity. These two cells apparently have different characteristics, but their deformability would be evaluated as the same by conventional approaches due to the same transit time. In order to distinguish these cells, we propose a new evaluation parameter, *equilibrium velocity*, by focusing on the cell motion when they are in equilibrium during the transit. Cell viscosity is a time-dependent property¹, so that the response damped out when a cell reaches equilibrium. Therefore, we can focus on only the time-independent properties, such as cell stiffness, by using equilibrium velocity. In the case of Fig. 2.1b and c, the equilibrium velocity of the cell on the top of Fig. 2.1b is slower than the lower one by comparing the corresponding slopes of the linear segment from their motion profiles. Assuming the same amount of deformation in the channel, we can say that the cell with greater equilibrium velocity has better deformability.

The observability of stiffness-based deformability is introduced based on the newly proposed parameter. Since the cell stiffness is directly related to the equilibrium velocity, we define the stiffness-based deformability of a cell as observable when its equilibrium velocity is measurable. The sufficient and necessary number of sensing points to evaluate cell stiffness are discussed.

Experimental study is conducted on the RBCs from a healthy subject and a diabetic patient. Two phases, the phases of deformation and equilibrium, were

¹ The time-dependent property of viscosity is sometimes referred as *rate-dependant*.

Fig. 2.1 **a** A series images of a RBC through a microchannel under a microscope. **b** Two cells pass through identical microchannels with the same transit time. The ellipsoids represent cell locations at the same time intervals. **c** The motion profiles of cells in Fig. 2.1b. The transit time for two RBCs through the channel are the same while the motion profiles are different



experimentally observed from the motion profiles. Dimensional analysis is performed on the basis of the stiffness-related parameters, and three dimensionless parameters for determining stiffness-based deformability are derived. Finally, a new dimensionless \widehat{DI} is introduced by combining three dimensionless parameters, and the difference between the evaluation using transit time and \widehat{DI} is compared and shown based on the experimental results.

The rest of the chapter is organized as follows: Firstly, a brief review on related works is presented in Sect. 22.2. The observation and physics behind the cell behavior through a microchannel is explained in Sect. 22.3. After that, the observability of cell stiffness is introduced in Sect. 22.4, and it is followed by the experimental study in Sect. 22.5. The experimental results are discussed by using the newly introduced dimensionless \widehat{DI} in Sect. 22.6. Finally, the chapter is concluded in Sect. 22.7.

2.2 Related Works

The mechanical properties of cells have been used as biomarkers for cell biophysics [10]. Various methods have been developed for evaluating the deformability of biological cells [11–17]. These methods can be categorized into direct and indirect methods based on the nature of sensing techniques. The direct methods are the ones evaluating cell properties by the response of cells while directly applying an external force onto them with an instrument, such as an atomic force microscope (AFM) [17, 16] and optical tweezers [5, 12, 14]. For examples, Radmacher et al. measured the viscoelastic properties of human platelets with an AFM [18]. Dao et al. studied on the mechanics of human red blood cells by optical tweezers [19].

On the other hand, the indirect methods are the ones evaluating cell properties based on cell behavior without giving a direct excitation. One of the first works were done by Worthen et al. [20]. Isermann et al. measure nuclear mechanics in [21]. Tsukada et al. measured the deformability of RBCs in diabetes mellitus [4]. Adamo et al. assessed cell deformability by sensing the travel time of a cell through a narrow passage by the electrical impedance of cells [8]. Youn et al. studied the deformability of RBCs by using an array of orifices [22]. Zheng et al. developed a high-throughput measurement for RBCs [6]. Tomaiuolo et al. analyzed the membrane viscoelasticity of RBC membrane based on the relation between fluid pressure and cell velocity [13]. Hou et al. studied the deformability of breast cancer cells using a microchannel [7]. Byun et al. characterized the deformability and surface friction of cancer cells [23]. Gossett et al. evaluated cell mechanical properties based on hydrodynamic stretching and cell deformation [24]. In our former works, the transit time of a cell through a microchannel was used for the evaluation of cell stiffness [25]. An observation of two-phase motion of cells through a microchannel from experiments is shown in [26]. Later, a method for separating two phases was proposed in [27], and the comparison between cell stiffness evaluated by the equilibrium velocity and average velocity is discussed in [28]. The concept of observability is firstly mentioned in [29].

In this chapter, we conducted experiments on a healthy subject and a diabetic patient. Moreover, we present the dimensional analysis to obtain a dimensionless index of cell stiffness-based deformability for general microchannel system.

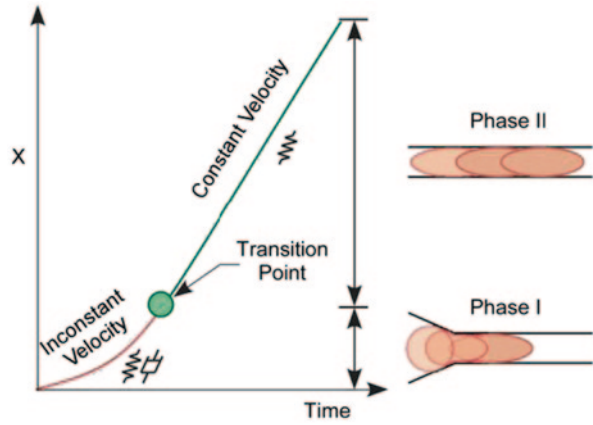
2.3 The Stiffness-Based Deformability

General motion profile of a cell through a microchannel is illustrated in Fig. 2.2. The profile can be separated into two parts based on the motion profile. The first part is when the cell just enters the channel, and cell velocity varies with time. The second part is when the cell eventually reaches a new equilibrium state, and the velocity becomes constant. The motion profiles in first and second part are illustrated by a curve and a line in Fig. 2.2. According to the difference of cell motion before and after reaching the equilibrium, we define the cell as in Phase I and Phase II during the transit, respectively.

It is well-known that most of biological cells have the properties of viscoelasticity [30]. Hence, a cell can be modeled by mechanical elements, such as springs and dampers, for representing cell stiffness and viscosity, respectively. From the viewpoint of mechanics, the force response of a deformed spring, F_k , is the function of its stiffness, k , and deformation, δ_k , which is

$$F_k = k\delta_k \quad (2.1)$$

Fig. 2.2 General cell behavior inside a microchannel can be separated into two phases, Phase I and II. Two phases are represented by an exponentially increasing curve and a straight line, respectively



The force response of a deforming damper, F_c , is a function of the damping coefficient, c and deformation rate, $\dot{\delta}_c$ which is

$$F_c = c\dot{\delta}_c \text{ where } \dot{\delta}_c = \frac{d\delta_c}{dt} \quad (2.2)$$

The overall force response of a deformed viscoelastic material would be the resultant of both the responses in Eqs. (2.1) and (2.2). When a cell reaches equilibrium, every deformation, δ_k and δ_c , remains constant. Thus, the response of cell stiffness remains constant, and the response of cell viscosity becomes zero.

For example, Kelvin-Voigt model is one of classic viscoelastic models, and it represents viscoelastic response by a spring and a damper connected in parallel. In the case of Kelvin-Voigt model, the total force response would be the sum of Eqs. (2.1) and (2.2), which is

$$F = F_k + F_c \quad (2.3)$$

Also, the deformation of the spring and damper are synchronized because of parallel connection, and that gives $\delta_k = \delta_c = \delta$. While a cell is deformed to enter a narrow channel, $\delta \neq 0$ and $\dot{\delta} \neq 0$, thus $F_k \neq 0$ and $F_c \neq 0$. It means that the cell motion is affected by both cell stiffness and viscosity. When the deformation is concluded and the cell reaches to equilibrium, $\delta \neq 0$ and $\dot{\delta} = 0$, thus $F_k \neq 0$ and $F_c = 0$. As a result, the cell viscosity no longer affects the cell motion, and, its stiffness can be solely evaluated from the equilibrium state. Based on the idea, stiffness-based deformability is defined as follows:

Definition 1

Stiffness-based deformability is defined as the deformability of a cell when it is in equilibrium, where only the stiffness affects its motion but not the viscosity.

2.4 Observability of Cell Stiffness in Microchannel system

The observability of a microchannel system is defined as

Definition 2

Stiffness-based deformability of a cell is observable if equilibrium velocity of a cell inside a microchannel is measurable.

The purpose for introducing the concept of observability is to minimize the resources needed for the evaluation of stiffness-based deformability. To measure the equilibrium velocity of a cell requires continuous tracking of the cell through a microchannel as the method explained in [27]. The question then arises as to how many sensing points are necessary and sufficient in order to measure the equilibrium velocity of a passing cell? The *sensing point* here represents the locations where the position sensors are implemented as in an actual setup. The sensors are capable of detecting a passing cell, thus the time, T_i of a passing cell at the location, X_i , of the sensor can be recorded for position analysis, where i indicates the i -th sensing point.

It is not possible to measure the velocity of a cell in a microchannel with one sensor. Therefore, two sensing points are definitely necessary. Let's consider system variables shown in Fig. 2.3 and two cases shown in Fig. 2.4a and b. Since it is impossible to determine the transition point by just 2 points, as shown in Fig. 2.4a, the equilibrium velocity, u_{eq1} , cannot be obtained. It means that the cell stiffness-based deformability cannot be evaluated by two sensing points, and the cell stiffness-based deformability is not observable.

Nevertheless, two sensing points can still be enough to evaluate cell stiffness under a special case when

$$\frac{D_c}{\lambda_m} \rightarrow 0 \quad (2.4)$$

Equation (2.4) represents the channel length, λ_m , is much longer than cell diameter, D_c , as shown in Fig. 2.4b. The ratio between the duration of Phase I and Phase II is small enough so that Phase I can be neglected. It implies that

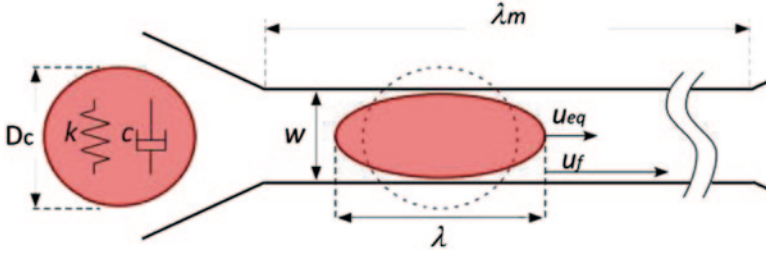


Fig. 2.3 The parameters of a microchannel system.

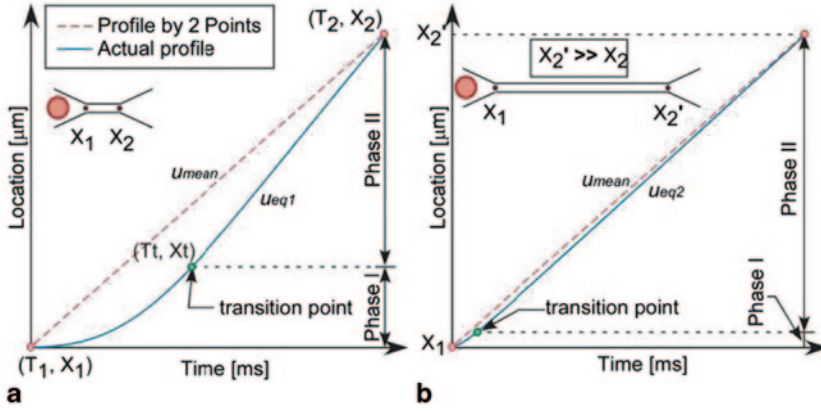


Fig. 2.4 **a** The mean velocity, u_{mean} and equilibrium velocity, u_{eq} are obviously different since the velocity varies significantly while the cell enters the channel. **b** $u_{mean} \rightarrow u_{eq}$ when the channel length approaches infinity, which makes the effect of transient responses insignificant [29]

$$\frac{X_t}{\lambda_m} \approx 0 \text{ and } (T - T_t) \approx T \quad (2.5)$$

Where T_t and X_t are the time and location of the transition point where a cell concludes to a new equilibrium state. The equilibrium velocity can be written as

$$\begin{aligned} u_{eq2} &= \lim_{\substack{\frac{X_t}{\lambda_m} \rightarrow 0 \\ \lambda_m}} \frac{\lambda_m - X_t}{T - T_t} \\ &= \lim_{\substack{\frac{X_t}{\lambda_m} \rightarrow 0 \\ \lambda_m}} \frac{1 - \frac{X_t}{\lambda_m}}{\frac{T}{\lambda_m} - \frac{T_t}{\lambda_m}} \\ &= u_{mean} \end{aligned} \quad (2.6)$$

From Eq. (2.6), we have that the equilibrium velocity equals the mean velocity, u_{mean} under the condition of Eq. (2.5). It shows that the two sensing points are sufficient in this special case. The results lead to the following Theorem

Theorem 1

Stiffness-based deformability of a cell is observable by two sensing points if $(D_c / \lambda_m) \rightarrow 0$

Next, in the case of three sensing points, an additional sensing point is included, and it can be used as a checking point for examining if three points, (T_1, X_1) , (T_2, X_2) and (T_3, X_3) , are on the same line. If the three points are on the same line, it say that the cell has reached equilibrium. Accordingly, another theorem about observability of cell stiffness with three sensing points is

Theorem 2

For cases, **except** $(D_c / \lambda_m) \rightarrow 0$, three sensing points are necessary and sufficient for judging whether a cell is in equilibrium or not.

As an extension to Theorem 2, three or more sensing points are sufficient for judging if the stiffness-based deformability of a tested cell is observable.

2.5 Experiments

2.5.1 Experimental Setup and Configuration

Figure 2.5 shows the experimental system. A microscope (Olympus Ltd.) is equipped with a high-speed vision system (Photron Inc.), where the shutter speed and the spatial resolution of the system are 500 ns and 0.24 μm , respectively. A microfluidic chip is fabricated with microchannels inside it. The dimension of the channel is 30 μm in length, 4 μm in height and 4 μm in width, as shown in Fig. 2.6. The velocity of the flow inside the channel is controlled by adjusting the pressure difference between the inlet and outlet of the microchannel as shown in Fig. 2.7. When the pressure difference increases, the flow rate increases, and vice versa.

RBCs are obtained from two subjects, a diabetic patient (male, 50 s) and a healthy subject (male, 30 s). The subjects have read and signed the consent for the experiment before the experiment. The blood was withdrawn from the subjects by a licensed doctor 30 min before the experiments.

Fig. 2.5 The experimental setup includes a microfluidic chip, a microscope, a high-speed camera and a computer. A microchannel is fabricated inside the microfluidic chip

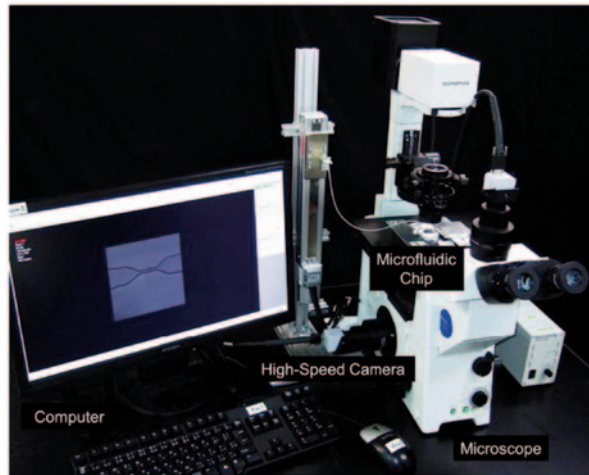


Fig. 2.6 The dimensions of the microchannel used in the chapter are shown here

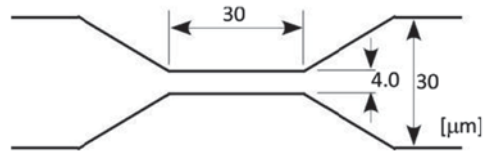
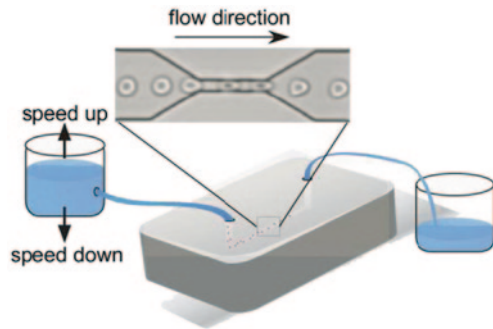


Fig. 2.7 The flow inside a microchannel is directly controlled by the pressure difference between the pressure at the inlet and outlet of the microfluidic chip [29]

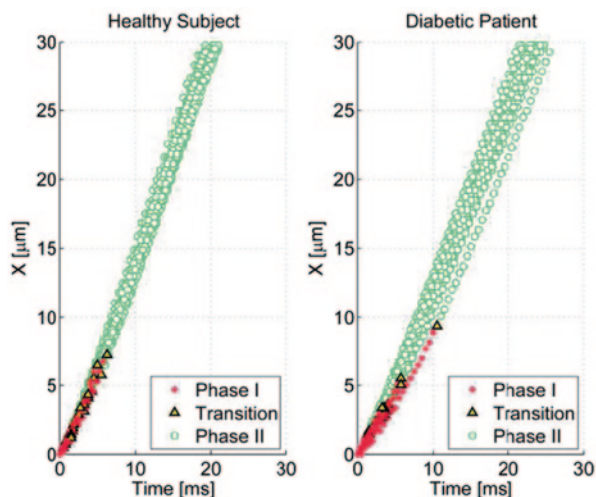


2.5.2 Experimental Procedure

The step-by-step experimental procedure is listed as follows:

1. RBCs are acquired 30 min before the experiment. The blood is kept in vacuum tubes avoiding any interaction with air.
2. Standard saline solution washed through the microchannel before the experiment for making sure there is no air in the channel as well as for keeping the surface condition as similar as possible between different tests.

Fig. 2.8 The cell motion profiles of the healthy subject (*left*) and the patient (*right*). The cell motion inside the microchannel is separated into two phases by the method proposed in [27]. Data points in Phase I are in *red*, and the ones in Phase II are in *green*. Black markers indicate the transition point of each profile



3. The blood is diluted with the same saline solution at the ratio of 1/50. After that, the blood-saline mixture is injected into the microchannel from the inlet.
4. The flow inside the microchannels is directly controlled by the pressure different between the inlet and outlet of the microfluidic chip as shown in Fig. 2.7. The actual flow rate for each experiment is calculated based on cell motion using the method developed in [31].
5. The high-speed vision system is set to focus on the microchannel area where the channel width is $4.0\ \mu\text{m}$ in the experiment², and cell motion through the channel is recorded at the prescribed frame rate, 2000 fps.
6. After finishing capturing images from the high-speed vision system, the images are processed by MATLAB with the toolbox of image processing for tracking the motion of RBCs. The information of the time and location of each RBC through the microchannel are measured and recorded.

2.5.3 Experimental Results

The motion profiles of RBCs through the microchannel for both the healthy subject and diabetic patient are plotted in Fig. 2.8. Each motion profile is divided into two phases by the method proposed in [27], and the red, green and black markers represent the data points in Phase I, II and the transition point, respectively. The cell flow-in velocity, as average cell velocity over the cross-sectional area before

² The width of $4.0\ \mu\text{m}$ is chosen since RBCs are generally ranged from $6\text{--}8\ \mu\text{m}$ in diameter. The microchannel should be narrow enough to deform the cell but not too narrow to cause damages. Moreover, based on our experience, RBCs are easily stuck in the microchannels with width $3\ \mu\text{m}$ or less.

entering the channel [31], are 0.26 $\mu\text{m/ms}$ and 0.20 $\mu\text{m/ms}$ for the tests with the RBCs of the healthy subject and the patient, respectively. The difference between the two flow-in velocities is within the error of the system, and will be normalized for a fair evaluation in the later analysis.

2.6 Discussion

2.6.1 Dimensional Analysis

For evaluating stiffness-based deformability of a cell by a microchannel system, a functional relation among the physical quantities of the system and the cell is assumed as follows³:

$$F(k, D_c, \lambda, u_{eq}, u_f, w, \mu) = 0 \quad (2.7)$$

where k , D_c , λ , u_{eq} , u_f , w and μ are cell stiffness, cell undeformed diameter, cell in-channel length, equilibrium velocity, fluid velocity⁴, channel width and fluid viscosity, respectively. The friction coefficient of contact is not included in Eq. (2.7) because it is assumed no direct contact between a cell and channel wall, and the interaction between them is always through a thin layer of fluid, which is as known as *Thin-Film Lubrication Theory*. (see details in Appendix A and [32]) The quantities are indicated in Fig. 2.3. The units of these 7 dimensional quantities are:

$$k \sim [FL^{-1}], D_c \sim [L], \lambda \sim [L], u_{eq} \sim [LT^{-1}], u_f \sim [LT^{-1}], w \sim [L], \mu \sim [FL^{-1}T]$$

where [F], [L] and [T] are fundamental dimensions, and are force, length and time, respectively. Buckingham π theorem [33] is adopted for solving the dimensionless parameters of the system. The dimensional matrix is

$$\mathbf{M} = \begin{bmatrix} 1 & 0 & 0 & 0 & 0 & 0 & 1 \\ -1 & 1 & 1 & 1 & 1 & 1 & -2 \\ 0 & 0 & 0 & -1 & -1 & 0 & 1 \end{bmatrix} \quad (2.8)$$

The rows correspond to the dimensions [F], [L] and [T], and the columns correspond to the dimensional quantities k , D_c , λ , u_{eq} , u_f , w and μ . Since the system has 7 dimensional quantities and the rank of the dimensional matrix is 3, we are looking for 4 dimensionless parameters⁵ from Eq. (2.8). The dimensionless parameters can be obtained by letting

³ see Appendix A for the details of how physical quantities are obtained.

⁴ fluid velocity here represent the velocity of fluid inside the channel when there is no cell in the channel. The fluid velocity is estimated based on the velocity profile as the method described in [31].

⁵ the value of 4 is obtained by subtracting the rank, 3, from the total number of dimensional quantities, 7.

Hyper Bio Assembler for 3D Cellular Systems

Arai, T.; Arai, F.; Yamato, M. (Eds.)

2015, XI, 349 p. 202 illus., 161 illus. in color., Hardcover

ISBN: 978-4-431-55296-3